



## Multi-variable approach to determine treatment efficiency of wetland: size effect and electro-kinetic effects

Sandeep Gupta<sup>a,\*</sup>, Rattandeep Singh<sup>a</sup>, Prodyut Ranjan Chakraborty<sup>a</sup>, R.K. Sharma<sup>a</sup>, A.B.O. Soboyejo<sup>b</sup>, Xiaohua Wei<sup>c</sup>, Anand Plappally<sup>a</sup>

<sup>a</sup>Mechanical Engineering Department, Indian Institute of Technology Jodhpur, Jodhpur, Rajasthan, India, email: [pg201271009@iitj.ac.in](mailto:pg201271009@iitj.ac.in) (S. Gupta)

<sup>b</sup>Department of Mechanical and Aerospace Engineering, The Ohio State University, Columbus, OH, USA

<sup>c</sup>Maritime Research Centre and School of Civil and Environmental Engineering, Nanyang Technological University, Singapore, Singapore

Received 31 March 2014; Accepted 16 June 2014

---

### ABSTRACT

Empirical stochastic multi-variable models for prediction of treatment efficiency of wetlands are presented in this article. Wetlands of seven different shapes are visualized using tracer studies. Two different variants of experiments are carried out. Numerous flow rate variations are performed keeping surface area of the wetland constant. The experiment is also carried out with a variation in volume of the wetland which helps to study the effect of flow height on the hydrodynamics within the wetland. A multi-variable model for treatment efficiency in terms of change in tracer concentration as a function of shape, volumetric height of water within the wetland, time, and mass flow rate is considered. Further, another set of experiments is performed studying the treatment efficiency in terms of electro-kinetic parameters. This involves measuring the pH, turbidity, temperature, electrical conductivity, total dissolved salts at inlet and outlet and residence time with varying flow rate, and height of water for the seven different wetland models under study. The electro-kinetic parameters changes due to difference in concentration of the tracer dye which simulates impurities. In this case, treatment efficiency is expressed as a function of the above-discussed electro-kinetic variables, time variation, water height, as well as variation in the mass flow rate. The stochastic multi-parameter models, thus, empirically derived in the above two cases have high coefficient of determination. The models thus derived may be used as a tool for quick analysis of treatment efficiency of any shape and size of a three-dimensional wetland.

*Keywords:* Multi-parameter approach; Electro-kinetic; Wetland; Tracer; Treatment; Acrylic model; Regression

---

\*Corresponding author.

*Presented at the Conference on Desalination for the Environment: Clean Water and Energy 11–15 May 2014, Limassol, Cyprus*

## 1. Introduction

Lagoons, ditches, marshes, bogs, and swamps are fresh water resources or wetlands that play an important role in ground water recharge, water treatment, and sedimentation as well as ecological management [1]. Constructed ponds of shallow depth ranging from 0.9 to 1.5 m are termed as oxidation ditches or sewage stabilization ponds or lagoons [2]. This is very low-cost wastewater treatment device [2]. Developing nations like India should have sustainable solutions which serve as a base for future generations and are also available to them in the long run. Places such as Rajasthan which are also regions of high-petroleum reserves can also use wetlands for treatment of produced water [3]. The wetlands are a low-energy low-cost treatment with an energy consumption of 0.12 Kwh/m<sup>3</sup> and cost estimates in the range 0.006–12.6 US \$/m<sup>3</sup>, respectively, for produced water treatment [4,5].

Treatment in wetlands in principles occurs as a result of time and conditions available for settling of suspended impurities, oxidation of materials, metabolic microbial growth, chemical breakdown by sunlight, as well as nutrient uptake by plants species which may grow within and specific to the wetland and its geospatial location [6,7]. Wetlands are free surface and sub-surface according to aerobic and anaerobic conditions as well as open to atmosphere and those not open, respectively [7]. The efficiency of treatment is dependent on impurity occurrences, time of interaction between the pollutants within a specific volume, and the microbial processes if any [8]. To maximize treatment, it is pertinent to minimize short circuiting [9,10]. The existence of preferential flow paths within the wetland is known as short circuiting [8]. These allow passage of certain dissolvable materials to pass through the wetland faster than the actual time for interaction provided by the system [8]. It is to be kept in mind that the residence time calculation is volumetric, ignoring constructions within the wetland, recirculation zones, and flow gradients [8].

Wetland reservoir sub-irrigation systems (WRSIS) and farmland channel wetland system (FCWS) are systems which work in tandem with recycling agricultural wastewater; thus, encouraging waste water reuse [11]. Further work through theoretical approach on improving the efficiency of the wetland within the FCWS was performed by Wei et al. [10]. In this, the shape of the existing wetland was changes keeping the surface area constant. This work also hinted on the control of the flow characteristics in order to improve residence time and in turn treatment [12]. Different shapes of wetland may have variable influence on the treatment efficiency [12].

Wetlands reduce nutrient content in agricultural farm effluent in case of WRSIS and FCWS. Industrial wastewater such as palm oil effluents are treated by reducing the chemical oxygen demand and well as total suspended solids using wetlands [13]. In these studies, shallow wetland topography is considered which may help in providing the treatment due to the dominant frictional forces [14]. The major aspect which decides the type of treatment is also the depth of the water in the wetland. Therefore, the variation of depth or height of water is also discussed within this study.

There are numerous dye tracer studies on wetlands [15]. Tracer impacts the prediction of fluid transport [16]. Measurements are to be performed throughout the experiment to maintain the accuracy or authenticity of the tracer studies [16]. Most of the studies have used Rhodamine as a desired tracer for residence time experiments due to its low toxicity, background interferences adsorption rates, and large time range for degradation [8,17]. In this study, Rhodamine is being used for the tracer tests.

When a dye is introduced at a specific location to the water, it simulates point source pollution of the water. Hence, when a dye is introduced into the wetland model in order to uncover its hydrodynamics, it also plays its role as an impurity which may impact the chemistry of water. In this way, the specific volume of water under consideration becomes a dilute solution with increasing concentration of contaminants with time. This is also the case in FCWS wetland discussed by Wei et al. [10], but not discussed or thought about. The measurement of pH, electrical conductivity, total dissolved solids, and turbidity will help in ascertaining the extent of contamination or contaminant removal too from these wetlands. It is also true that variation of pH between the inlet and the outlet will also help in characterizing the efficiency of the transport within the wetlands.

An experiment conducted in Idaho Springs-Central City mining district of Colorado looked at metal removal efficiencies of wetlands from an acid mine drainage [18]. The experiment showed that with change in the flow rate there was a reduction in metal concentration and an increase in pH [18]. This would mean that variation in pH may be a function of flow rate and concentration of the contaminant metal.

Other indicators for assessing wetland treatment efficiency are specific conductance and turbidity [19]. It should be observed that ephemeral wetlands do show substantial time-based variation in water chemistry due to shallow nature and changing water levels [20]. This may also indicate that indicators of specific conductance and turbidity may vary with depth of water.

Theoretical work by Singh et al. [21], confirms the results of empirical work performed in this paper.

## 2. Materials

In this study, wetland models are constructed using acrylic transparent sheet. These models are constructed such that height of inlet and outlet can be varied. One model of 50 cm × 50 cm × 50 cm is constructed with three levels of inlet and outlet at the height of 15.5, 30, and 45.5, respectively. The image of the experimental wetland model is shown in Fig. 1. Dimension of inlet and outlet at the three different heights is 10 cm × 1.5 cm. Position of the inlet and outlet kept on the hypotenuse of 50 cm × 50 cm. This is performed supposing that water should travel the longest available distance before it gets discharged at outlet. A small reservoir is made at the back of the inlet so that any disturbance caused by the silicon tubing can be minimized.

Another model with same configuration is shown in Fig. 2 but different base dimension of 64 cm × 64 cm is used. Two geometrically similar obstructions are created in model such that base surface area in contact with water is same with initial model in Fig. 1. The shape of these obstructions is cylindrical. These are kept within the 64 cm × 64 cm wetland model at suitable positions (Tables 1 and 2).

Controlled inflow of water is maintained in the wetland models using peristaltic pump (Ravel Hiteks Pvt Ltd model RH-120LS) having a flow range of 100–5000 ml/min. The other peristaltic pump (Ravel Hiteks Pvt Ltd model RH-P100VS-100-PC) with a smaller flow range of 0–100 ml/min is used for the injection of the dye. Tetraethylrhodamine (Rhodamine B) dye having pH in the range 6.5–9.5, molecular weight 479.01, and chemical formula  $C_{28}H_{31}ClN_2O_3$  is used as a tracer during the entire sets of experiments.



Fig. 1. An acrylic wetland model with dimension of 50 cm × 50 cm × 50 cm.

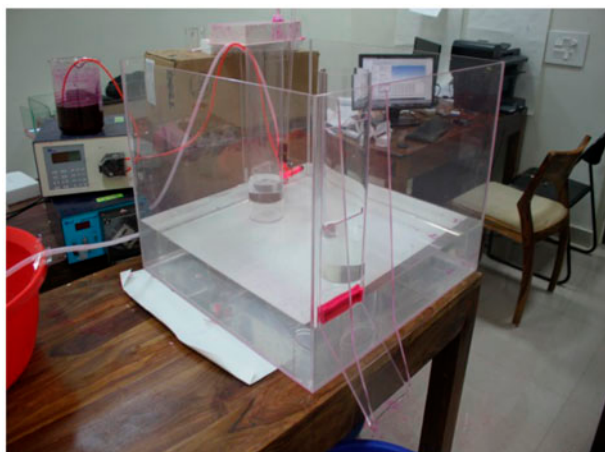


Fig. 2. An acrylic wetland model with dimension of 64 cm × 64 cm × 50 cm.

Various electro-kinetic parameters are measured using Multi-parameter Tester (model Eutech PCSTEST35-01X441506/Oakton 35425-10) and Turbidimeter (EUTECH instruments, model Turbidimeter TN-100).

Tracer is pre-processed by mixing the Rhodamine B dye (1 g) with small volume of concentrated HCl solution (5 ml) in 1,800 ml of water. pH value of solution is adjusted so that the stability of Rhodamine can be maintained. Organic dye like Rhodamine is used in the experiments because of its nontoxicity and low density comparing with other dyes [21].

## 3. Experimental methodology

Various sets of experiments are performed in acrylic wetland models manufactured here. They are performed by varying the height of the position at inlet and outlet, mass flow rate of water, and changing the size of wetland model. Hydrodynamic study on these models is performed by varying the parameters mentioned above and their effect on electro-kinetic parameters.

Initially, water is filled up to the particular height and proper time is given so that water can become still. Experiments are done at three flow rates of 150, 300, and 500 ml/min so that they cover a wide range of slow flows through wetlands.

Before starting the experiment, caution was exercised for stagnation of water within the models. Local turbidity in wetland volume causes the diffusion of tracer within the wetland leading to error in readings. Peristaltic pump is used to attain a specific inflow of water. Once the water gains momentum the dye is introduced. This is done to simulate the mixing of point impurity sources in large flowing wetlands at a very slow speed. Individual experiments are

Table 1

Variation of pH across the 50 cm × 50 cm × 50 cm geometry as a function of change in conductivity  $X_1$ , change in total dissolved solids  $X_2$ , and change in turbidity  $X_3$  at specific time intervals  $X_4$  at an inflow rate of 500 ml/min

Predictor variables	$a$	$b_1$	$b_2$	$b_3$	$b_4$	$R^2$	$S$
$X_1, X_2, X_3, X_4$	1.799	-0.06567	-0.02986	0.244	-0.0009	95.29%	0.042

Table 2

Variation of pH across the 50 cm × 50 cm × 50 cm geometry as a function of change in conductivity  $X_1$ , change in total dissolved solids  $X_2$ , and change in turbidity  $X_3$  at specific time intervals  $X_4$  at an inflow rate of 300 ml/min

Predictor variables	$a$	$b_1$	$b_2$	$b_3$	$b_4$	$R^2$	$S$
$X_1, X_2, X_3, X_4$	1.4812	-0.03514	-0.06328	-0.296	0.000265	95.50%	0.052

performed for each of the specific inflow and outflow levels discussed above.

Water samples are collected at the outlet at regular time intervals. Initially, a pipette was used to deliver the dye. But it was observed that the initial flow of dye from the pipette cannot be maintained with level of the dye decreasing the pipette. Therefore, peristaltic pump is again used to introduce the dye into the inlet.

In this experiment, samples are collected at the interval of 30 s initially and then time step was increased as the experiment proceeds. These time steps were 60 s, 120 s, and 240 s, respectively. The experiment culminates once the variation of pH at the outlet is negligible. At each of the interval time steps, a sample of effluent water is collected throughout the experiment.

During the experiment, temperature and light are controlled and kept within the range of 22–25 °C. Darkness or negligible light was used to prevent photolysis of Rhodamine B. Sample collected from the outlet is examined within a short period of time at the same place for various parameters like pH, electrical conductivity, total dissolved solute, and turbidity. Same set of readings taken for various flow rate, height, and size.

#### 4. Results and discussion

The experiments are conducted in a 50 cm × 50 cm wetland acrylic model. Fig. 3 shows a shallow flow happening at an inlet with a head of 15.5 cm with a mass flow rate of 100 ml/min. The transport of the dye at the fifth minute from the start of the inflow is shown. This also showed that apart from short circuiting that is taking place the flow path was being followed by Rhodamine B.

Further development of the flow at 100 ml/min observed after 15 min showed recirculation near to the



Fig. 3. Rhodamine B tracers at the fifth minute in 50 cm × 50 cm × 50 cm model at 15.5 cm level of water.

outlet. Further, the recirculation zone was spread over a large area on the left-hand top corner.

Similar studies for the 64 cm × 64 cm were performed and Rhodamine B tracers at 5 min after initiation of tracer was observed and enumerated as shown in Fig. 4.

The plots in Figs. 3 and 5 enumerated flow behavior of 50 cm × 50 cm × 50 cm wetland configuration with a water head of 15.5 cm (Fig. 6). The pH variation in this configuration at the same head but at different flow rates is enumerated in Fig. 7. There is an overall decrease in pH with time. In the meanwhile, it is also observed from Fig. 7 that for inflow rates of 150 and 300 ml, at approximately around 1,000 s after introduction of the dye the variation pH of the effluent tends to subside.

It is observed that with increase in volume of water within the 50 cm × 50 cm × 50 cm configurations it takes lesser time for the pH to stabilize at the outlet. This can be clearly illustrated by comparing the

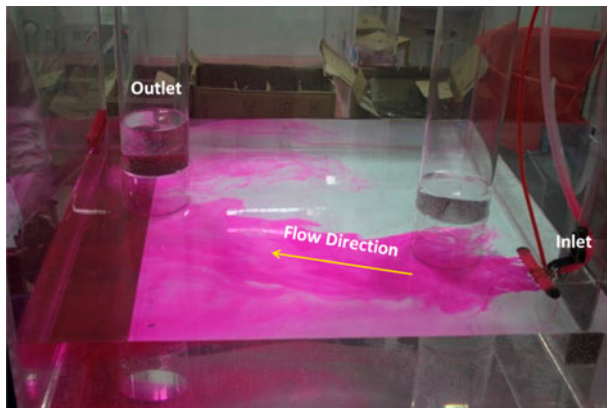


Fig. 4. Rhodamine B tracers at the 15th minute in 50 cm × 50 cm × 50 cm model at 15.5 cm level of water.

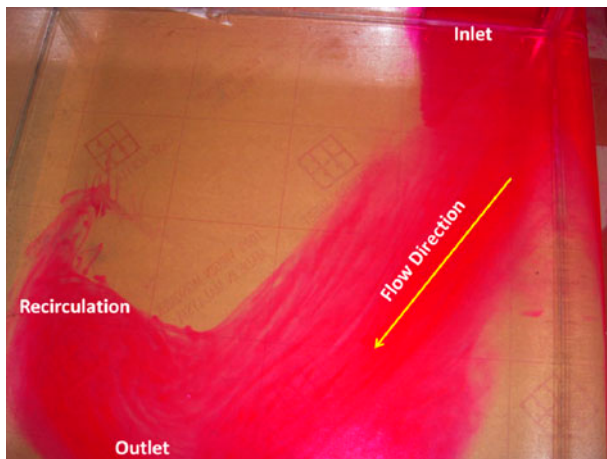


Fig. 5. Rhodamine B tracers at the fifth minute in 64 cm × 64 cm × 50 cm model at 15.5 cm level of water.

pH variation as a function of time for same inflow rates but in varying volumetric scenarios as represented in Figs. 7–9. It is observed that irrespective of the dye flow rates the stagnation in variation of the effluent pH occurs at approximately the same time at a 45.5 cm head.

Another major observation is that for the geometry in Figs. 7–9, irrespective of the volume of the configuration 300 ml/min appears as the dye flow rate which helps in abrupt reduction of the pH with time. This also means that there exists a specific concentration of inflow which can be optimally treated at a faster rate by a specific geometry. This is also confirmed from the work by Singh et al. [21]. Therefore, it is pertinent to analyze and model the behavior according to the specific volume.

The effluent turbidity is measured along with other electro-kinetic parameters with change in time. It is

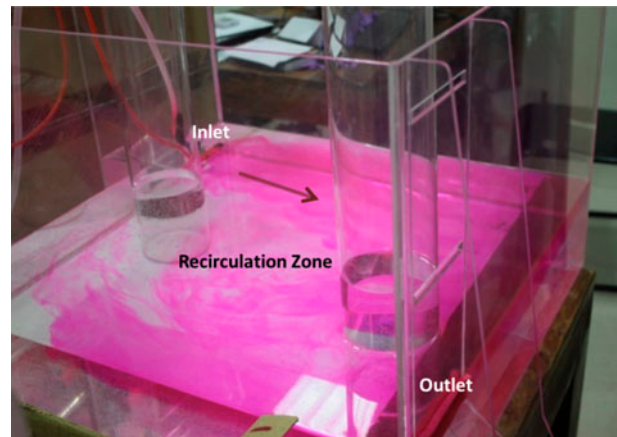


Fig. 6. Rhodamine B tracers at the 15th minute in 64 cm × 64 cm × 50 cm model at 15.5 cm level of water, showing recirculation in between the two constructed island cylinders.

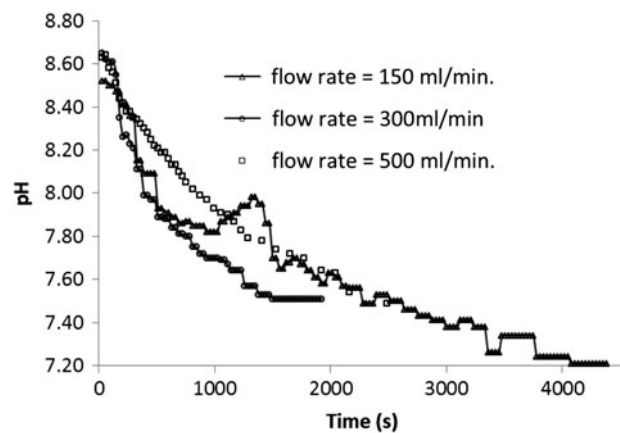


Fig. 7. The variation of effluent pH with time at different dye flow rates for a wetland configuration 50 cm × 50 cm with 15.5 cm head.

found to have no specific linear relationship with pH. For a water head for 30 and 45.5 cm, the pH is plotted as a function of turbidity and is illustrated in Figs. 10 and 11. For the benefit of the case study, performed experiment is also performed for 15.5 cm.

## 5. Analysis of dye inflow for a wetland head of 15.5 cm

At the event of high flows, the variation in pH is dependent on how much turbid the wetland is. Secondly, from the plots illustrated in Figs. 7–9, almost a linear relation between pH and time is observed.

From the point of view of thermodynamics of irreversible processes, flux of mass may disturb a

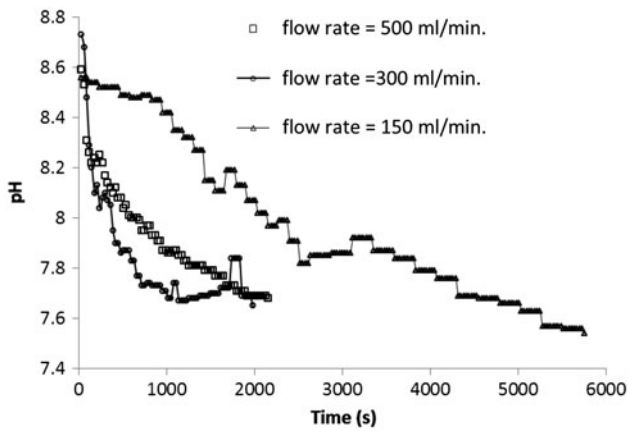


Fig. 8. The variation of effluent pH with time at different dye flow rates for a wetland configuration 50 cm × 50 cm × 50 cm with 30.0 cm head.

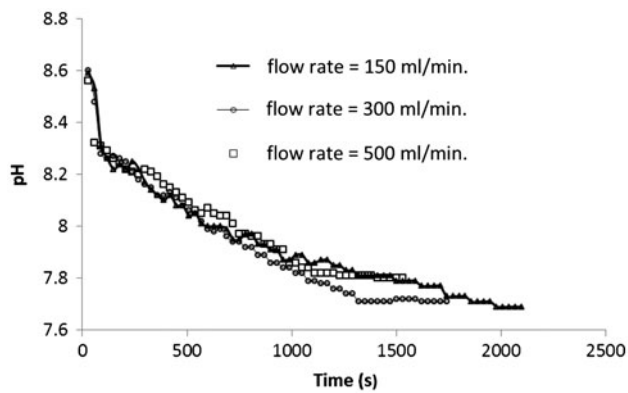


Fig. 9. The variation of effluent pH with time at different dye flow rates for a wetland configuration 50 cm × 50 cm × 50 cm with 45.5 cm head.

statistical equilibrium [23]. There is a linear relationship between the fluxes and corresponding gradients that may influence each other [24]. The gradients in this study are related to change in conductivity  $X_1$ , change in total dissolved solids  $X_2$ , and change in turbidity  $X_3$  that may affect change in pH,  $Y$ , for the total treatment process and will not lose their inter-dependence with time [25]. This can be expressed as:

$$\Delta Y \approx a + b_1 X_1 + b_2 X_2 + b_3 X_3 + b_4 X_4 \quad (1)$$

In this study, the Eq. (1) can be used as a regression equation. But for regression is performed with only independent variables. It is clear that the  $X_i$ 's do not lose their inter-dependence till the process ends. In order to remove the interdependence, mathematical correlations between the  $X_i$ 's are removed mathematically [25]. The elaborate procedure for mathematically removing interdependence is not in the scope of this paper. Interested researchers are advised to refer elsewhere [25]. Once the eigenvalues and eigenvectors imbibing the correlations between change in conductivity  $X_1$ , change in total dissolved solids  $X_2$ , change in turbidity  $X_3$ , and specific time interval  $X_4$  are removed, the remaining matrix contains independent corresponding variables  $V_1, V_2, V_3$ , and  $V_4$ , respectively. Regression of variation in pH is performed against these newly derived independent  $V_i$ 's.

The variation of pH as a function of independent variables is expressed as:

$$\Delta \text{pH} = 0.53649 + 0.09459 V_1 - 0.0438 V_2 + 0.1016 V_3 - 0.0187 V_4 \quad (2)$$

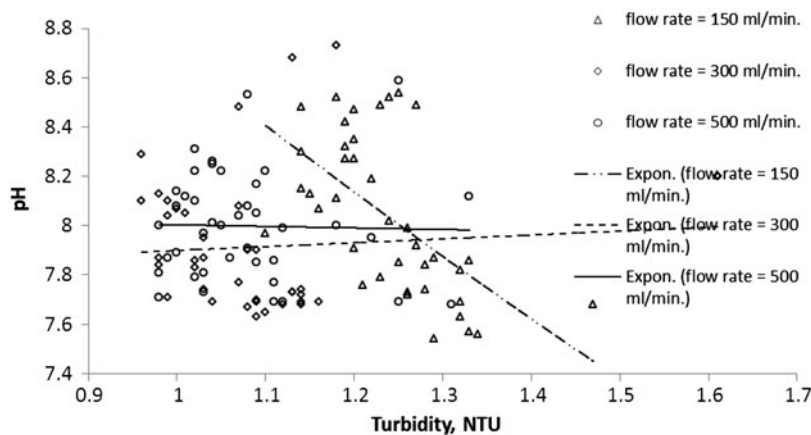


Fig. 10. Variation of pH as a function of turbidity at a wetland water head of 30.0 cm.

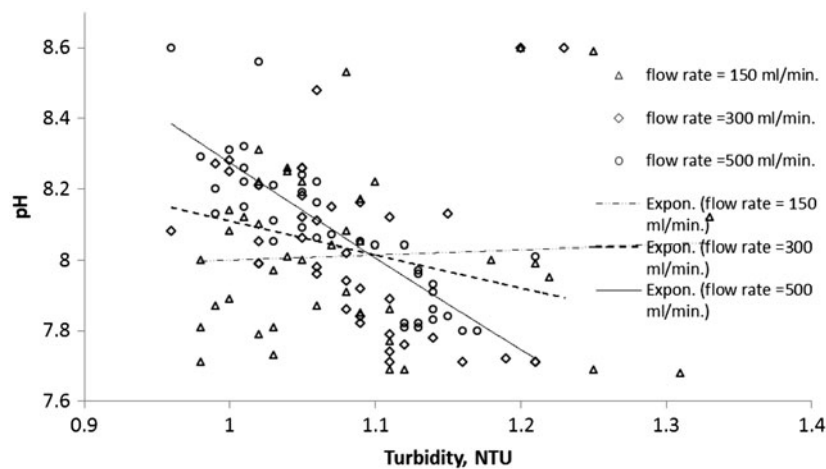


Fig. 11. Variation of pH as a function of turbidity at a wetland water head of 45.5 cm.

It should be noted that high velocities may initiate turbulence and thus increasing the surface area interaction with the bottom topography. This process may churn out the settling impurities making the wetland turbid. The individual influence of the turbidity on the variation of pH is enumerated by Eq. (2). Here, Eq. (2) has a coefficient of prediction  $R^2$  value of 95.29% and an error in the model of 0.042.

Similarly, calculation is performed for an inflow rate of 300 ml/min. Similar to Eqs. (2) and (3) also elaborates the positive dependence of pH on the turbidity within the wetland model.

The variation in effluent pH as a function of new independent variation in conductivity  $V_1$ , change in dissolved solids  $V_2$ , change in turbidity  $V_3$ , and time  $V_4$  is predicted with a coefficient of determination  $R^2$  of 95.5% and error in the model is 0.052.

$$\Delta\text{pH} = 0.58395 - 0.12148 V_1 - 0.07804 V_2 + 0.0493 V_3 - 0.0259 V_4 \quad (3)$$

With decrease in flow rate, the proposed regression equation is found to lose its prediction capability. This is clear from Table 3. One major aspect that becomes clear is that with slow transport the pH variation is very much dependent on the local conductivity of the water as well as large amount of time; the water and dye have time to interact with each other.

The variation in pH is predicted with an  $R^2$  value of 77.55% and error  $S$  of 0.109, as:

$$\Delta\text{pH} = 0.5991 + 0.1197 V_1 - 0.0051 V_2 - 0.0049 V_3 + 0.0401 V_4 \quad (4)$$

## 6. Analysis of dye inflow for a wetland head of 30.0 cm

From the above analysis, it is found that Eq. (1) is a good predictor of the chemical transport happening within the wetland. This would mean that Eq. (1) can be a good predictor of similar case studies. With decrease in height, the predictability of the model is weak for flow of 500 and 300 ml/min flow rates. This is clear from Tables 4 and 5. The pH variation as a function of turbidity is provided in Fig. 11 for use in statistical calculations to arrive at regression equations in Table 4.

It is found that the independent influence of the time is positive while conductivity, amount of dissolved salts, and turbidity negatively influence the pH change.

$$\Delta\text{pH} = 0.5991 - 0.1213 V_1 - 0.0051 V_2 - 0.0086 V_3 + 0.0073 V_4 \quad (5)$$

Table 5 provides a very feeble relationship between the variation of pH and other parameters with a low  $R^2$  value of 35.68%. Hence, Eq. (1) may not work effectively of 300 ml/min inflow rate through an inlet at 30 cm above the assumed bottom topography of the wetland.

$$\Delta\text{pH} = 0.9654 + 0.0828 V_1 + 0.0737 V_2 + 0.076 V_3 + 0.165 V_4 \quad (6)$$

This is not the case with low inflow rates at this height of 30 cm of water head. Since the flow is relatively slow, the conductivity and total dissolved solids

Table 3

Variation of pH across the 50 cm × 50 cm × 50 cm geometry as a function of change in conductivity  $X_1$ , change in total dissolved solids  $X_2$ , and change in turbidity  $X_3$  at specific time intervals  $X_4$  at an inflow rate of 100 ml/min

Predictor variables	$a$	$b_1$	$b_2$	$b_3$	$b_4$	$R^2$	$S$
$X_1, X_2, X_3, X_4$	1.050	-0.0347	-0.020	-0.0088	0.002292	77.55%	0.109

Table 4

Variation of pH across the 50 cm × 50 cm × 50 cm geometry as a function of change in conductivity  $X_1$ , change in total dissolved solids  $X_2$ , and change in turbidity  $X_3$  at specific time intervals  $X_4$  at an inflow rate of 500 ml/min

Predictor variables	$a$	$b_1$	$b_2$	$b_3$	$b_4$	$R^2$	$S$
$X_1, X_2, X_3, X_4$	1.143	-0.0269	-0.0397	0.009	0.1028	79.02%	0.105

Table 5

Variation of pH across the 50 cm × 50 cm × 50 cm geometry as a function of change in conductivity  $X_1$ , change in total dissolved solids  $X_2$ , and change in turbidity  $X_3$  at specific time intervals  $X_4$  at an inflow rate of 300 ml/min

Predictor variables	$a$	$b_1$	$b_2$	$b_3$	$b_4$	$R^2$	$S$
$X_1, X_2, X_3, X_4$	-1.89	0.0389	-0.0331	0.249	0.00157	35.68%	0.234

will play a big role in influencing the pH existing within the wetland. This is illustrated from Table 6.

Reaffirmation of the prediction capacity of the model for wetlands handling low flows at 30 cm is observed from Eq. (7) which predicts the change in pH with great accuracy as illustrated in Table 6.

$$\Delta\text{pH} = 0.4131 + 0.1863 V_1 + 0.0172 V_2 - 0.0762 V_3 - 0.1056 V_4 \quad (7)$$

From the above discussions, it is clear that Eq. (1) can be a good candidate for the prediction of variation of wetland assessment parameters. This can be tested performing the analysis of dye inflow for a wetland head of 15.5 cm. Here, two cases of 500 ml/min as well as 300 ml/min are tested and elaborated in Table 7, Eq. (8), Table 8, and Eq. (9). It should be noted that experimental turbidity values for the two cases are provided in Fig. 12.

For 500 ml/min dye flow rate, Eq. (1) was able to assess the variation of pH as a positive influence from conductivity and turbidity.

$$\Delta\text{pH} = 0.5182 + 0.1707 V_1 - 0.0529 V_2 + 0.0048 V_3 - 0.0355 V_4 \quad (8)$$

The variation of pH was supported by a coefficient of determination of only 59.20% in case of 30 cm head of water.

$$\Delta\text{pH} = 0.563 - 0.1142 V_1 - 0.1281 V_2 - 0.0939 V_3 - 0.698 V_4 \quad (9)$$

## 7. Variation of pH as a function of total process time within 50 cm × 50 cm × 50 cm wetland with 45.5 cm water

The linearity that exists between the pH and cumulative time that is very much clear from Figs. 7–9. Using this linearity as a regression equation, it is possible to derive constant “ $p$ ” for each of the flow rates which may help to calculate the process constant for a specific head of water. The generalized equation for  $\Delta\text{pH}$  ( $Y_{\text{pH}}$ ) can be written as:

Table 6

Variation of pH across the 50 cm × 50 cm × 50 cm geometry as a function of change in conductivity  $X_1$ , change in total dissolved solids  $X_2$ , and change in turbidity  $X_3$  at specific time intervals  $X_4$  at an inflow rate of 100 ml/min

Predictor variables	$a$	$b_1$	$b_2$	$b_3$	$b_4$	$R^2$	$S$
$X_1, X_2, X_3, X_4$	0.5211	-0.0182	-0.0730	-0.0025	0.000711	93.87%	0.084

Table 7

Variation of pH across the 50 cm × 50 cm × 50 cm geometry as a function of change in conductivity  $X_1$ , change in total dissolved solids  $X_2$ , and change in turbidity  $X_3$  at specific time intervals  $X_4$  at an inflow rate of 500 ml/min

Predictor variables	$a$	$b_1$	$b_2$	$b_3$	$b_4$	$R^2$	$S$
$X_1, X_2, X_3, X_4$	3.31	-0.02249	-0.0669	0.127	0.004494	86.24%	0.097

Table 8

Variation of pH across the 50 cm × 50 cm × 50 cm geometry as a function of change in conductivity  $X_1$ , change in total dissolved solids  $X_2$ , and change in turbidity  $X_3$  at specific time intervals  $X_4$  at an inflow rate of 300 ml/min

Predictor variables	$a$	$b_1$	$b_2$	$b_3$	$b_4$	$R^2$	$S$
$X_1, X_2, X_3, X_4$	0.4828	0.02112	-0.0365	0.454	0.002714	59.90%	0.206

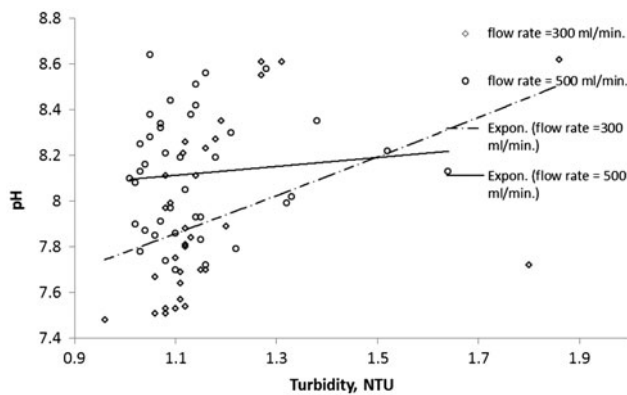


Fig. 12. Variation of pH as a function of turbidity at a wetland water head of 15.5 cm.

$$Y_{pH} \approx p + m_1 X_t \tag{10}$$

Tables 9–11 represent the model fit by applying the Eq. (10) on the data enumerated in Figs. 7–9.

In summary, for the wetland of 45.4 cm height, the pH change can be predicted as a function of the cumulative time  $X_t$  and processing constant  $X_c$ . Here, the new variable processing constant  $X_c$  is derived from the individual constants “ $p$ ” derived from Tables 9–11, respectively, and arranged in a column along the other variables of time and flow rate [25]. Then, from Eq. (10),  $\Delta pH (Y_{pH})$  can be expressed as:

Table 9

The variation in effluent pH as a function of the cumulative process time  $X_t$  at a flow rate of 500 ml/min

Predictor variable	$p$	$m_1$	$R^2$	$S$
$X_t$	0.2744	0.000404	91.27%	0.055

$$Y_{pH} \approx p + m_1 X_t + m_2 X_c \tag{11}$$

As per the assumptions, the change in flux will be influenced by interdependent parameters. The same framework as discussed earlier is used to remove the correlation if any between cumulative time  $X_t$  and processing constant  $X_c$ . The new independent variables are  $V_{1t}$  and  $V_{2c}$  which correspond to  $X_t$  and  $X_c$ , respectively.

$$\Delta pH = 0.5745 + 0.04009 V_{1t} - 0.1906 V_{2c} \tag{12}$$

Thus, it is found that pH change is positively influenced by time. This is true since addition of dye is performed, simulating point source impurity addition in wetlands. From Table 12, it shows that Eq. (11) can predict the variation in pH with high coefficient of prediction. Hence, it is implied that this model can predict similar case studies with high accuracy.

In order to test the predictability of this model as illustrated in Eqs. (11) and (12), it is applied in a case

Table 10

The variation in effluent pH as a function of the cumulative process time  $X_t$  at a flow rate of 300 ml/min

Predictor variable	$p$	$m_1$	$R^2$	$S$
$X_t$	0.2783	0.000451	88.78%	0.076

Table 11

The variation in effluent pH as a function of the cumulative process time  $X_t$  at a flow rate of 150 ml/min

Predictor variable	$p$	$m_1$	$R^2$	$S$
$X_t$	0.3356	0.000313	83.09%	0.090

Table 12

Variation of pH as a function of cumulative time  $X_t$  and processing constant  $X_c$  at a head of 45.5 cm

Predictor variables	$p'$	$m_1$	$m_2$	$R^2$	$S$
$X_t, X_c$	0.4363	0.000368	-0.435	84.41	0.083

Table 13

The variation in effluent pH as a function of the cumulative process time  $X_t$  at a flow rate of 500 ml/min

Predictor variable	$p$	$m_1$	$R^2$	$S$
$X_t$	8.2644	-0.00031	83.49%	0.09

Table 14

The variation in effluent pH as a function of the cumulative process time  $X_t$  at a flow rate of 300 ml/min

Predictor variable	$p$	$m_1$	$R^2$	$S$
$X_t$	0.0312	0.000156	91.88%	0.091

Table 15

Variation of pH as a function of cumulative time  $X_t$  and processing constant  $X_c$  at a head of 30.0 cm

Predictor variables	$p$	$m_1$	$m_2$	$R^2$	$S$
$X_t, X_c$	0.1415	0.0000108	0.94001	99.66%	0.22

study of variation of pH as a function of total process time within 50 cm × 50 cm × 50 with 30.0 cm water.

First, the simple model using Eq. (10) is elaborated. Table 13 provides linear relationship between cumulative process time and pH change in the effluent pH at a high flow of 500 ml/min with the high predictability  $R^2$  of 83.49% and low related error of modeling  $S = 0.09$ .

Similar prediction of variation in pH is derived as a function of cumulative time within the wetland with a dye inflow at 300 ml/min (Table 14). The predictability is quite optimal with Eq. (10).

Further, Eq. (11) is now applied for the prediction of variation of pH at a specific flow head irrespective of the flow rates 500 ml/min or 300 ml/min. Table 15 illustrates the high capability of the model.

Similar to Eq. (12), removal of interdependence between  $X_t$  and  $X_c$  is performed following the framework discussed above. Eq. (13) provides the independent influence of  $X_t$  and  $X_c$  for the effective prediction in dip in the pH that occurs with time.

$$\Delta\text{pH} = 4.3763 + 2.6179 V_1 - 2.8843 V_2 \quad (13)$$

## 8. Conclusions

New models for prediction of change in electrokinetic transport parameters within the wetland are shown.

- Irrespective of the flow rates the variation in pH can be measured. pH change is represented as a function of cumulative time spent by the dye within the wetland and new process constant.
- Irrespective of the shape and flow rate, pH change is a linear function of change in water conductivity, change in the dissolved solids, change in turbidity within the wetland, and time at each change.

Another major aspect is that there exists a specific concentration of dye inflow which can be optimally treated at a faster rate by a specific constructed wetland geometry.

## Acknowledgment

The authors are indebted to the support of the Mr Ganpat Choudhary and Mr Mahesh from the Chemistry laboratory at IIT Jodhpur. The authors also take this opportunity to thank the administration of IIT Jodhpur for providing seed grant to support this work in 2014.

## References

- K. Subramanya, Engineering Hydrology, fourth ed., McGraw Hill Education (India) Private Limited, New Delhi, 2011.
- S.C. Rangwala, Water Supply and Sanitary Engineering, twenty-fifth ed., Charotar Publishing House Pvt. Ltd, Gujrat, 2011.
- B. Sheikh, Use of constructed wetlands for wastewater treatment and water recycling—Application to Saudi Arabian conditions, The Proceedings of Biological Treatment Forum at King Saud University, Riyadh, Saudi Arabia, May 16, 2011.
- A.K. Plappally, J.H. Lienhard V, Energy requirements for water production, treatment, end use, reclamation, and disposal, Renew. Sustainable Energy Rev. 16(7) (2012) 4818–4848.
- A.K. Plappally, J.H. Lienhard, Costs for water supply, treatment, end-use and reclamation, Desalin. Water Treat. 51 (2013) 200–232.
- M. King, Calculating photolysis rates and estimating photolysis lifetimes, ECGEB No. 1, RSC, Available from: [http://www.rsc.org/images/Environmental\\_Brief\\_No1\\_tcm18-235159.pdf](http://www.rsc.org/images/Environmental_Brief_No1_tcm18-235159.pdf).

- [7] WateReuse Research Foundation, Evaluate Wetland Systems for Treated Wastewater Performance to Meet Competing Effluent Water Quality Goals, Publication Number 05-006-1, WRF, Washington, DC, 2011.
- [8] D.B. Stairs, Flow Characteristics of Constructed Wetlands: Tracer Studies of the Hydraulic Regime, Thesis, Bio-resource Engineering Oregon State University, 1993.
- [9] G.R. Steiner, R. Freman, Configuration and substrate design for constructed wetlands in wastewater treatment, in: D.A. Hammer (Ed.), *Constructed Wetlands for Wastewater Treatment—Municipal, Industrial and Agricultural*, Lewis Publisher, Chelsea, MI, 1989.
- [10] X. Wei, X. Wang, B. Dong, X. Li, A.K. Plappally, Z. Mao, L.C. Brown, Simplified residence time prediction models for constructed wetland water recycling systems, *Desalin. Water Treat.* 51(7–9) (2013) 1494–1502.
- [11] X. Wei, A.K. Plappally, L.C. Brown, A.B.O. Soboyejo, B. Dong, Z. Mao, Numerical and multivariate stochastic approaches to characterize Guilin wetland dynamics, *Stoch. Environ. Res. Risk Assess.* 25(8) (2011), doi: 10.1007/s00477-011-0520-6.
- [12] J. Persson, N.L.G. Somes, T.H.F. Wong, Hydraulics efficiency of constructed wetlands and ponds, *Water Sci. Technol.* 40 (1999) 291–300.
- [13] N.A. Ariffin, Treatment of Industrial Wastewater using Constructed Wetland: Removal of Chemical Oxygen Demand (cod) and Total Suspended Solid (tss), Faculty of Chemical and Natural Resources Engineering Bachelor Thesis, Universiti Malaysia Pahang, 2009.
- [14] J. Kjellin, A. Wörman, H. Johansson, A. Lindahl, Controlling factors for water residence time and flow patterns in Ekeby treatment wetland, Sweden, *Adv. Water Resour.* 30 (2007) 838–850.
- [15] T. Headley, R.H. Kadlec, Conducting hydraulic tracer studies of constructed wetlands: A practical guide, *Ecohydrol. Hydrobiol.* 7(3–4) (2007) 269–282.
- [16] M.S. Field, Application of robust statistical methods to background tracer data characterized by outliers and left-censored data, *Water Res.* 45 (2011) 3107–3118.
- [17] M.D. Wahl, L.C. Brown, A.O. Soboyejo, J. Martin, B. Dong, Quantifying the hydraulic performance of treatment wetlands using the moment index, *Ecol. Eng.* 36 (2010) 1691–1699.
- [18] T.R. Wildeman, S.D. Machemer, R.W. Klusman, R.R.H. Cohen, P. Lemke, Metal removal efficiencies from acid mine drainage in the big five constructed wetland, Proceedings of the 1990 Mining and Reclamation Conference and Exhibition, Charleston, WV, April 23–26, 1990.
- [19] NEMA, Wetland Assessment and Monitoring Strategy for Kenya, National Environment Management Authority, Kenya, 2012.
- [20] C.J. Boeckman, J.R. Bidwell, Spatial and seasonal variability in the water quality characteristics of an ephemeral wetland, *Proc. Okla. Acad. Sci.* 87 (2007) 45–54.
- [21] R. Singh, S. Gupta, S. Raman, P. Sharma, P. Chakraborty, R.K. Sharma, L.C. Brown, X. Wei, A. Plappally, Comparative analysis of hydrodynamics of treatment wetlands using finite volume with empirical data, Conference and Exhibition on Desalination for the Environment: Clean Water and Energy, Grand Resort Hotel, Limassol, Cyprus, 11–15, 2014.
- [22] Y.M. Al-Riyami, Thermal Stability of Fluorescent Dyes as Geothermal Tracers, Thesis, Department of Petroleum Engineering of Stanford University, 1986.
- [23] L. Onsager, Reciprocal relations in irreversible processes II, *Phys. Rev.* 38 (1931) 2265–2279.
- [24] N.V. Churaev, Physical Chemistry of Mass transport Processes in Porous Bodies (in Russian), Chimija, Moscow 1990, 272.
- [25] A.K. Plappally, Theoretical and Empirical Modeling of Flow, Strength, Leaching and Micro-Structural Characteristics of V Shaped Porous Ceramic Water Filters, Dissertation, The Ohio State University, 2010, 244.